Generalized Automatic Modulation Classification for OFDM Systems Under Unseen Synthetic Channels

Sai Huang, *Senior Member, IEEE*, Jiashuo He, *Graduate Student Member, IEEE*, Zheng Yang, Yuting Chen, Shuo Chang, *Member, IEEE*, Yifan Zhang, and Zhiyong Feng, *Senior Member, IEEE*

***Abstract*— Automatic modulation classification (AMC) is a crucial technique for the design of intelligent transceivers and has received considerable research attention. Conventional feature-based (FB) methods have the advantage of low computational complexity. However, these methods are highly sensitive to the distribution shifts of the received signal caused by the variation of channel effects and have rarely been studied in orthogonal frequency division multiplexing (OFDM) systems under unseen synthetic channels with multipath fading effects, carrier frequency offset (CFO), phase offset (PO) and additive noise. To solve this problem, this paper proposes a novel FB method using the error vector magnitude (EVM) features for AMC tasks (termed as EVM-AMC), which can achieve reliable classification performance for the communication scenarios considering unseen synthetic channels in OFDM systems. Specifically, we first propose the axisymmetric mapping-based self-circulant differential division (AM-SCDD) algorithm to convert the received signal into the non-negative spectral quotient (NNSQ) sequence, deeply suppressing the synthetic channel effects. Subsequently, we derive the EVM features by analyzing the matched error vectors between the generated NNSQ sequence and the predefined NNSQ constellation symbol (NNSQCS) masks. During this process, a percentile-based filter is utilized to remove the outliers in each matched error vector. Finally, the feature samples collected from various channel conditions are sent to the multi-class support vector machine (SVM) classifiers for training and testing. Two candidate modulation type sets are employed to evaluate the performance of the proposed EVM-AMC method under both the constant and changing channel conditions. Our numerical results demonstrate that 1) the proposed method exhibits impressive robustness and generalization when dealing with unseen synthetic channels, 2) the proposed method yields the best classification performance when compared to the conventional FB AMC methods in the presence of channel effects.**

Manuscript received 16 October 2023; revised 22 February 2024; accepted 2 April 2024. Date of publication 16 April 2024; date of current version 12 September 2024. This work was supported in part by the National Natural Science Foundation of China under Grant 62171045, Grant 62201090, and Grant 62321001; in part by the Fundamental Research Funds for the Central Universities under Grant 2023RC16; and in part by Beijing University of Posts and Telecommunications (BUPT) Excellent Ph.D. Students Foundation under Grant CX2023233. The associate editor coordinating the review of this article and approving it for publication was X. Chen. *(Corresponding author: Shuo Chang.)*

The authors are with the Key Laboratory of Universal Wireless Communications, Ministry of Education, Beijing University of Posts and Telecommunications, Beijing 100876, China (e-mail: huangsai@bupt.edu.cn; jiashuohe@bupt.edu.cn; yz2016@bupt.edu.cn; cyting@bupt.edu.cn; changshuo@bupt.edu.cn; zhangyf@bupt.edu.cn; fengzy@bupt.edu.cn).

Color versions of one or more figures in this article are available at https://doi.org/10.1109/TWC.2024.3386762.

Digital Object Identifier 10.1109/TWC.2024.3386762

***Index Terms*— Automatic modulation classification, error vector magnitude, multipath fading channel, OFDM system.**

I. Introduction

AUTOMATIC modulation classification (AMC) is an intermediate process between signal detection and demodulation, which empowers the receiver to differentiate the modulation types of the received signal [1], [2]. It plays a pivotal role in various military and civilian applications, such as electronic warfare, cognitive radio, spectrum surveillance, spectrum management, and so on [3], [4], and [5].

Previous AMC methods can be grouped into two categories: likelihood-based (LB) methods [6], [7] and feature-based (FB) methods [8]. Traditional LB methods compare the likelihood ratio of each possible hypothesis against a threshold and provide the advantage of optimal solutions in the Bayesian sense [9]. However, they suffer from high computational complexity and are highly dependent on prior knowledge of channel conditions [10]. With the rapid development of deep learning (DL), current FB methods using the deep neural network (DNN) and convolutional neural network (CNN) for AMC has gained increasingly interests in both academia and industry [11], [12], [13], [14], as they can directly extract the discriminative modulation information and then provide high classification accuracy. However, the DL based FB methods require to collect massive well-labeled data for model training and they are also computational-intensive. For recognizing the modulation types in a low computational cost manner, this work gives a special focus on the conventional FB methods, which usually require extracting certain features from the received signal such as cyclostationary characteristics [15], instantaneous features [16], high-order cumulants (HOC) [17], and their combinations [18]. Although lots of FB AMC methods have been investigated in many scenarios, this task is still very challenging for real-world applications [19].

In practical wireless communication systems, the received signal often experiences the effects of multipath propagation induced by reflections, diffractions, and scattering [20]. Due to its great ability against severe channel conditions, orthogonal frequency division multiplexing (OFDM) is widely applied in modern wireless communication systems [21]. As a result, the AMC tasks for OFDM signal are of great significance for the design of intelligent transceivers in the future [22].

Previous research efforts of AMC have made remarkable achievements under additive white Gaussian noise (AWGN) channel [23], [24], [25], [26], [27], [28]. However, the AMC task with unknown channel conditions hasn't been well studied in current works, especially for OFDM systems. Since the multipath fading effects can severely distort the received signal and introduce uncertainties, most existing AMC works usually exhibit significant performance degradation in such scenarios due to bad channel generalization. For this reason, some initial AMC works considering the channel effects are developed by researchers for OFDM systems [29], [30], [31], [32], [33], [34], [35], [36].

To improve the classification accuracy in the presence of the channel effects, Shih et al. proposed an efficient AMC technique using HOC [31], where a blind channel estimation method was employed to combat the channel effects during the feature extraction process. However, the process of channel estimation is complex and the classification performance is highly related to the accuracy of estimated channel information. Wang et al. in [32] proposed a convolutional neural network (CNN) based AMC method in multiple-input and multiple-output (MIMO) systems, where the zero-forcing (ZF) equalization technique was adopted to enhance the classification performance. However, this equalization-based method is computation-consuming and also performs less well with imperfect channel state information. In [33], Gupta et al. investigated a blind AMC method for OFDM system over frequency-selective fading environments, where the normalized fourth-order cumulants of the fast Fourier transform (FFT) of both the received signal and its square were extracted as the modulation-specific features. However, this algorithm suffers from high computational complexity due to the use of the Taylor series in the cumulants estimation. In [34], Huynh-The et al. proposed a symbolwise OFDM modulation classification network, which employed the data reconstruction to against the channel deterioration. However, this method is only evaluated on the dataset with four modulation types and the same channel conditions. To sum up, these methods [31], [32], [33], [34] can achieve excellent classification performance under certain channel conditions, but if the channel conditions are different between the runtime and training stage, they may suffer a significant performance deterioration [35]. To deal with this problem, recently we proposed a spectral quotient cumulants-based AMC method [36], which employed the spectral circular shift division algorithm to resist the channel effects [37]. However, this method performs badly in the low signal-to-noise (SNR) region and the received signal model hasn't taken the carrier frequency offset (CFO) and phase offset (PO) into consideration. Thus, there is still an urgent need to develop a reliable and generalized AMC method for OFDM systems with unseen channel conditions.

In this paper, we propose an error vector magnitudes-based AMC (EVM-AMC) method to achieve reliable classification performance under unseen synthetic channels.[1] An extensive pool of modulation types including binary phase shift keying (BPSK), quadrature PSK (QPSK), 8PSK, 16PSK, 8 quadrature amplitude modulation (QAM), 16QAM, 32QAM, 64QAM, 4 amplitude shift keying (ASK) and 8ASK can be well classified via the proposed method. The main contributions are summarized as follows.

- We proposed a novel EVM-AMC method that is applicable to OFDM systems. Compared to other FB methods, our method achieves superior classification accuracy when dealing with unknown synthetic channels.
- We presented the axisymmetric mapping-based self-circulant differential division (AM-SCDD) algorithm to construct the non-negative spectral quotient (NNSQ) sequence. The resistance of the NNSQ sequence to the variation of the CFO, PO and channel effects guarantees the robustness of the proposed method.
- We proposed an EVM-based feature extractor, which exploits the modulation-specific information from the matched error vectors between the generated NNSQ sequence and the predefined NNSQ constellation symbol (NNSQCS) masks. To keep the statistical stability of the EVM features, we employed a simple percentile-based filter to remove the outliers in each error vector.

The rest of this paper is structured as follows. Section II describes the OFDM signal model and formulates the AMC task in this paper. Section III provides the detailed process of the proposed EVM-AMC method. In Section IV, the experimental setup is introduced in detail. The numerical results and discussions are given in Section V. Finally, we conclude this paper in Section VI.

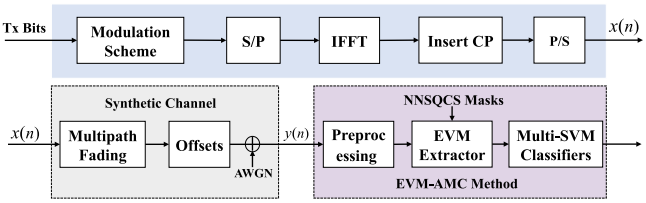

Fig. 1. OFDM baseband system with the proposed EVM-AMC method.

II. Preliminaries

In this section, we first introduce the OFDM signal model considering the synthetic channels with multipath fading effects, CFO, PO, and additive noise. Then, for ease of understanding, we formulate the AMC problem caused by the change of channel conditions in detail.

A. Signal Model

The overall baseband single-input single-output OFDM system is given in Fig. 1, where the proposed EVM-AMC algorithm is applied at the receiver side. In the transmitter, the binary bits are first modulated by a predefined modulation scheme to generate OFDM symbol with N_0 subcarriers, i.e., $\overline{\boldsymbol{X}}_m = [\overline{X}_m(0), \ldots, \overline{X}_m(k), \ldots, \overline{X}_m(N_0-1)]^T$. After performing N-point inverse fast Fourier transform (IFFT), the

[1] In this paper, the synthetic channel effects are defined as the joint effects of the multipath fading channel, AWGN, CFO and PO.

n^{th} baseband OFDM signal of the m^{th} symbol is denoted as

$$x_m(n) = \frac{1}{N}\sum_{k=0}^{N-1} X_m(k)e^{j2\pi kn/N}; \\ -N_g \le n \le N-1, \tag{1}$$

where $N = \rho N_0$ and ρ is the oversampling factor; N_g is the length of the cyclic prefix (CP); $X_m(k)$ is the modulated signal at the k^{th} subcarrier and can be expressed as

$$X_m(k) = \begin{cases} \overline{X}_m(k), & 0 \le k \le N_0/2 - 1 \\ \mathbf{Z}, & N_0/2 \le k \le N_0(\rho - 1/2) \\ \overline{X}_m(k_1), & N_0(\rho - 1/2) - 1 \le k \le N-1, \end{cases} \tag{2}$$

where $k_1 = k - N_0(\rho - 1)$ and $\mathbf{Z}$ is the zero padding vector.

After passing through the synthetic channel, the m^{th} received signal impaired with multipath fading, offsets, and AWGN can be represented as [33]

$$y_m(n) = e^{j(2\pi\Delta f_m n/N + \Phi_m)}\sum_{l=1}^{L} h_{l,m}x_m(n-\tau_l) + w_m(n), \\ -N_g \le n \le N-1, \tag{3}$$

where Δf_m is the frequency offset normalized by the subcarrier spacing $1/T$ (T is an OFDM symbol interval); Φ_m denotes the phase offset within $(-\pi, \pi)$; $w_m(n)$ is the AWGN and $h_{l,m}$ is the l^{th} channel tap with delay τ_l of total L in the m^{th} transmission. For a Rayleigh multipath fading channel, the fading coefficient of each path can be denoted as $h_{l,m} = \sqrt{P_l}v_{l,m}$, where P_l is the expected variance in the l^{th} tap and $v_{l,m} \sim \mathcal{CN}(0,1)$ is a complex Gaussian variable. As for a Rician channel, there is a line of sight (LOS) component in the first tap, hence $h_{1,m} = \sqrt{P_1}(\sqrt{K_f} + v_{1,m})/(\sqrt{K_f + 1})$ [38], where K_f is the Rician-K-factor.

B. Problem Formulation

The objective of AMC is to extract the discriminating information from the received signal for recognizing the modulation types. Conventional AMC research attention focuses on identifying the modulation types of the samples in the testing dataset that were collected or generated under the same channel conditions as the training dataset. However, due to the variation of channel environments, it is unrealistic to assume that both the training and testing samples suffer from the same channel effects in practice. Hence, as shown in Fig. 2, the AMC problem in this paper is formulated as follows.

Assuming $\mathcal{D} = \{(\boldsymbol{y}_m, \Theta_m)\}_{m=1}^{N_m}$ is the training dataset collected under a specific synthetic channel condition $\mathcal{H}(\cdot)$, where N_m is the total number of samples and Θ_m is the corresponding modulation scheme employed in $\boldsymbol{y}_m$. With the aid of the training dataset $\mathcal{D}$, a well-trained classifier $\mathscr{C}(\cdot)$ can be obtained for the subsequent inference.

Considering a different channel condition $\mathcal{H}'(\cdot)$ during the runtime, the receiver will first capture a signal $\boldsymbol{y}'_m$ modulated by Θ'_m and then feed it into the classifier $\mathscr{C}(\cdot)$ for prediction. Thus, the predicted result can be denoted as

$$\hat{\Theta}'_m = \mathscr{C}(\boldsymbol{y}'_m). \tag{4}$$

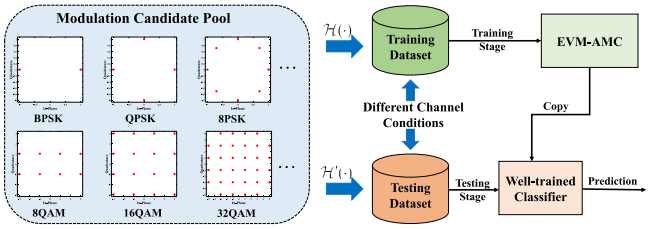

Fig. 2. Overview of an AMC problem caused by different channel conditions.

where $\hat{\Theta}'_m$ is the output of the classifier. Since the different channel conditions can lead to the distribution shifts between the training signal and the testing signal, $\hat{\Theta}'_m$ is probably different from Θ'_m. In other words, training an AMC model in certain channel conditions while applying it to different channel conditions will lead to performance deterioration. Therefore, a solution capable of training channel-agnostic classifiers is urgently needed for the AMC development.

III. Proposed EVM-AMC Method

In this section, we propose a novel AMC method for OFDM signals in the presence of unknown CFO, PO, noise, and channel effects. The architecture of this AMC method consists of three modules, namely signal preprocessing module, EVM-based feature extraction module, and multi-class support vector machine (SVM) classifier module. The detailed operations of our method are given below.

A. Signal Preprocessing

In a blind OFDM system, the OFDM parameters should be first estimated for the following AMC process. According to the cyclostationarity of the oversampled OFDM signals, the cyclic correlation function in [39] can be employed to estimate the OFDM sample length N, the CP length N_g as well as the oversampling factor ρ. To focus on the AMC methods itself, it is assumed that these parameters are known as a priori information in the subsequent process.

Considering the office and residential environments (small maximum delay scenarios), the CP duration can be two times the channel maximum delay. To avoid the CFO estimation errors caused by the multipath effects, we use the second half of CP to estimate the CFO value, which is given as [40]

$$\Delta\hat{f}_m = (1/2\pi)arg\{\sum_{n=-N_g/2}^{-1} y_m^*(n)y_m(n+N)\}, \tag{5}$$

where $(\cdot)^*$ denotes the conjugate operator and $arg\{\cdot\}$ denotes the inverse tangent function. After the CFO correction and the removal of CP, the output signal can be written as

$$\hat{y}_m(n) = e^{j(2\pi\varepsilon n/N + \Phi_m)}\sum_{l=1}^{L} h_{l,m}x_m(n-\tau_l) + \hat{w}_m(n), \\ 0 \le n \le N-1, \tag{6}$$

where ε is the residual normalized CFO value which is denoted as $\varepsilon = \Delta f_m - \Delta\hat{f}_m$; $\hat{w}_m(n)$ is the n^{th} additive noise after performing CFO correction.

Since the modulation-related information $\overline{\boldsymbol{X}}_m$ of the OFDM signal is in the frequency domain, we perform the FFT algorithm on the output signal

$$Y_m(k) = \sum_{k=0}^{N-1} \hat{y}_m(n) e^{-j2\pi kn/N}; \quad 0 \le k \le N-1. \tag{7}$$

After deleting the zero padding vector, we can obtain the frequency-domain vector $\overline{\boldsymbol{Y}}_m = [\overline{Y}_m(0), \ldots, \overline{Y}_m(k), \ldots, \overline{Y}_m(N_0-1)]^T$, whose element is denoted as

$$\overline{Y}_m(k) = \begin{cases} Y_m(k), & 0 \le k \le N_0/2 - 1 \\ Y_m(k_2), & N_0/2 \le k \le N-1, \end{cases} \tag{8}$$

where $k_2 = k + N_0(\rho - 1)$.

As studied in our previous work [41], the effects of channel frequency response (CFR) have high correlations at the neighboring subcarriers, which can be suppressed in a self-circulant differential division manner. Due to the linear transformation property of the FFT operation, the PO effect remains a constant on each subcarrier and can also be canceled by the operation of differential division. Considering the modulation constellation symbols are symmetric about the coordinate axes,[2] we propose the AM-SCDD algorithm to construct the NNSQ sequence $\overline{\boldsymbol{\Upsilon}}$ as

$$\overline{\boldsymbol{\Upsilon}} = [\overline{\boldsymbol{\Upsilon}}_{-S}, \overline{\boldsymbol{\Upsilon}}_{-S+1}, \ldots, \overline{\boldsymbol{\Upsilon}}_{-1}, \overline{\boldsymbol{\Upsilon}}_{1}, \ldots, \overline{\boldsymbol{\Upsilon}}_{S-1}, \overline{\boldsymbol{\Upsilon}}_{S}], \tag{9}$$

$$\overline{\Upsilon}_s(k) = |\Re\{\Upsilon_s(k)\}| + j|\Im\{\Upsilon_s(k)\}|, \tag{10}$$

$$\Upsilon_s(k) = \overline{Y}_m(k)/\overline{Y}_m(k_s), \tag{11}$$

where S is the maximum self-circulant shift step, $|\cdot|$ is the absolute operator, $\Re\{\cdot\}$ and $\Im\{\cdot\}$ denote the real and imaginary operators, respectively, k_s is the index of the denominator, which is the remainder after division of $k-s$ by N_0. For simplicity, the detailed operations of the AM-SCDD are summarized in Algorithm 1.

Let $\boldsymbol{\Theta} = \{\Theta_i\}_i^I$ denote the candidate modulation type set of total I. Then, the ideal NNSQ values of Θ_i can be obtained when $\overline{Y}_m(k)$ and $\overline{Y}_m(s_k)$ are the constellation symbols of Θ_i. After iterating over the set of $\boldsymbol{\Theta}$, we can easily obtain the NNSQCS masks set of different modulation types, which is denoted as $\{\overline{\boldsymbol{\Upsilon}}_{\Theta_i}\}_i^I$. As illustrated in Fig. 3, we can find that the modulation-specific information can be well preserved in the new signal representation. In the following, we will introduce the approach to extract the features for AMC task.

B. EVM-Based Feature Extractor

EVM is a popular figure-of-merit adopted by various communication standards for evaluating the distortions in a communication system [42]. Since the matched error vectors between the generated NNSQ sequence and the predefined NNSQCS masks are highly related to the modulation type of the transmitted signal, we extract the EVMs from the matched error vectors as modulation-specific features.

[2]By performing the axisymmetric mapping scheme, the elements in each NNSQCS mask can be heavily reduced, thus reducing the computational complexity for the following feature extraction module.

Algorithm 1 Axisymmetric Mapping-Based Self-Circulant Differential Division (AM-SCDD)

Require: The length of OFDM signal: N; The m^{th} OFDM signal: $\boldsymbol{y}_m$; the length of CP: N_g; the oversampling factor: ρ; the maximum self-circulant shift step: S.
Ensure: The NNSQ sequence: $\overline{\boldsymbol{\Upsilon}}$;
1: Estimating the normalized CFO value via Eq. (5);
2: Correcting the received signal and then removing the CP to derive $\hat{\boldsymbol{y}}_m$ of length N;
3: Performing the FFT operation on $\hat{\boldsymbol{y}}_m$ to derive $\boldsymbol{Y}_m$;
4: Deleting the zero padding vector via Eq. (8);
5: **for** $s = -S$; $s \le S$; $s++$ **do**
6: **for** $k = 0$; $k \le N/\rho$; $k++$ **do**
7: Calculating the denominator index via $mod(k - s, N/\rho)$;
8: Generating the NNSQ signal of $\overline{\Upsilon}_s(k)$ via Eq. (10) and Eq. (11);
9: **end for**
10: **end for**
11: Merging the $\overline{\boldsymbol{\Upsilon}}_s$ vectors via Eq. (9);
12: **return** $\overline{\boldsymbol{\Upsilon}}$.

Firstly, the matched error vectors are derived as

$$\boldsymbol{e}_{\Theta_i} = |\overline{\boldsymbol{\Upsilon}} - \overline{\boldsymbol{\Upsilon}}^d_{\Theta_i}|, \quad 1 \le i \le I, \tag{12}$$

where $\overline{\boldsymbol{\Upsilon}}^d_{\Theta_i}$ is the decided symbol vector of $\overline{\boldsymbol{\Upsilon}}$ in terms of the NNSQCS mask $\overline{\boldsymbol{\Upsilon}}_{\Theta_i}$, and its k^{th} element can be given as

$$\overline{\Upsilon}^d_{\Theta_i}(n) = \underset{\Upsilon \in \overline{\boldsymbol{\Upsilon}}_{\Theta_i}}{\operatorname{argmin}} \left|\overline{\Upsilon}(n) - \Upsilon\right| \tag{13}$$

In order to stabilize the EVM features, we carry out a percentile-based outlier filter (POF) method to remove the outliers from each error vector. Due to the fact that the outliers are likely to be far away from the ideal NNSQ values, their error magnitude is much larger than that of the normal NNSQ value. According to this characteristic, given a specific percentile Q, we identify the top $Q\%$ largest numbers of $\boldsymbol{e}_{\Theta_i}$ as outliers and then filter them out. The filtered error vectors are denoted as

$$\boldsymbol{e}^f_{\Theta_i} = [e^f_{\Theta_i}(0), \ldots, e^f_{\Theta_i}(n), \ldots, e^f_{\Theta_i}(N_f - 1)]^T, \tag{14}$$

where N_f is the length of the filtered vectors.

Subsequently, we can extract the EVM from $\boldsymbol{e}^f_{\Theta_i}$ as

$$E_i = \sqrt{\frac{\sum_{n=1}^{N_f} (e^f_{\Theta_i}(n))^2}{N_f \overline{\Upsilon}^2_{max,\Theta_i}}}, 1 \le i \le I, \tag{15}$$

where $\overline{\Upsilon}_{max,\Theta_i}$ is the maximum amplitude of the elements in $\overline{\boldsymbol{\Upsilon}}_{\Theta_i}$. Finally, an EVM-based feature vector $\boldsymbol{\Xi} = [E_1, \ldots, E_i, \ldots, E_I]^T$ standing for the unknown modulation type is constructed and this ends the feature extraction module.

C. Multi-Class SVM Classifiers

The SVM is an efficient machine learning algorithm primarily used for classification tasks, which can find a hyperplane that best separates different classes in the feature space,

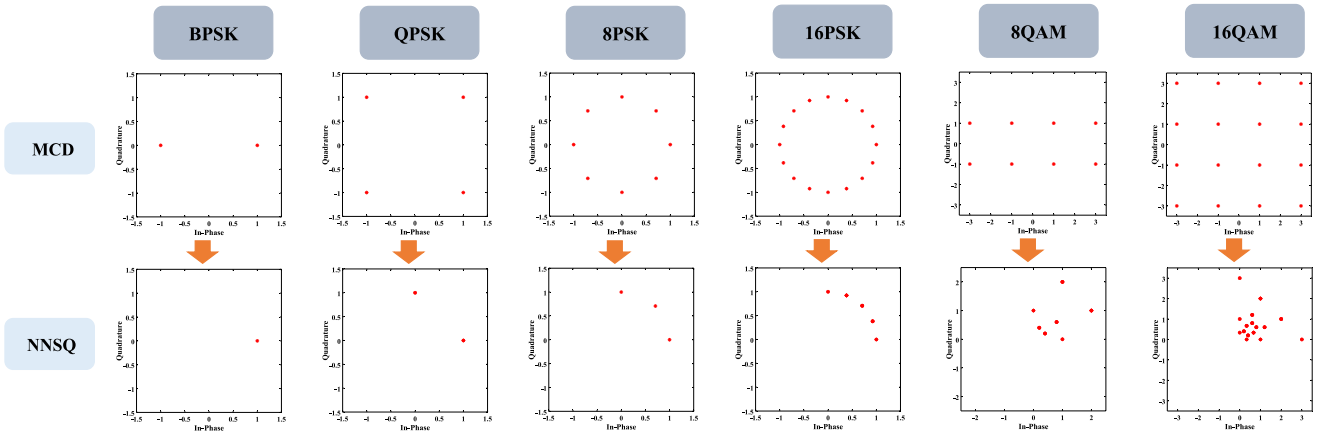

Fig. 3. The visualization of the NNSQ representation for different modulation types via constellation diagram; MCD is the abbreviation of modulation constellation diagram.

maximizing the margin between the classes [43]. To recognize multiple modulation types, we use the one-against-one strategy to train the multi-class SVM classifiers [44], [45]. Thus, a total of $I(I-1)/2$ two-class SVM classifiers need to be constructed.

Let $\boldsymbol{\Xi}_m^{N_i}, m = 1, \ldots, M$ and $N_i = 1, \ldots, I(I-1)/2$ denote the N_i^{th} training vectors in two classes (i.e., Θ_i and Θ_j) and $L_m^{N_i} \in \{-1, 1\}$ the corresponding one-hot encoded modulation type label. Then we train each binary SVM classifier by solving the primal optimization problem below [46]

$$\begin{aligned} \min_{\boldsymbol{w},b,\boldsymbol{\xi}} \quad & \frac{1}{2}\boldsymbol{w}^T\boldsymbol{w} + C\sum_{m=1}^{M}\xi_m \\ s.t. \quad & \begin{cases} L_m^{N_i}(\boldsymbol{w}^T\psi(\boldsymbol{\Xi}_m^{N_i}) + b) \geq 1 - \xi_m \\ \xi_m \geq 0, m = 1, \ldots, M, \end{cases} \end{aligned} \tag{16}$$

where $C > 0$ and ξ_m are the regularization and soft margin parameters; $\boldsymbol{w}$ and b are the weight vector and bias of the decision function; $\psi(\cdot)$ is the function to map the feature data into a higher-dimensional space. For solving Eq. (16), usually we can solve the following dual problem

$$\begin{aligned} \min_{\boldsymbol{\alpha}} \quad & \frac{1}{2}\boldsymbol{\alpha}^T K\boldsymbol{\alpha} - \boldsymbol{e}^T\boldsymbol{\alpha} \\ s.t. \quad & \begin{cases} \sum_{m=1}^{M} L_m^{N_i}\alpha_m = 0 \\ 0 \leq \alpha_m \leq C, m = 1, \ldots, M, \end{cases} \end{aligned} \tag{17}$$

where α_m is the coefficient associated with the m^{th} training sample; K is an M by M kernel matrix, whose element can be constructed as $K_{mn} = L_m^{N_i}L_n^{N_i}\psi(\boldsymbol{\Xi}_m^{N_i})^T\psi(\boldsymbol{\Xi}_n^{N_i})$. After solving Eq. (17), we can obtain the optimal $\boldsymbol{w}$ via the primal-dual relationship, i.e., $\boldsymbol{w} = \sum_{m=1}^{M} L_m^{N_i}\alpha_m\psi(\boldsymbol{\Xi}_m^{N_i})$. Then the decision function of the N_i^{th} SVM classifier is expressed as

$$SVM(\boldsymbol{\Xi}) = sgn(\boldsymbol{w}\psi(\boldsymbol{\Xi}) + b), \tag{18}$$

where $sgn(\cdot)$ denotes the sign fuction. After yielding the final predictions from total $I(I-1)/2$ SVM classifiers, we employ the voting method designed on the criterion of the max wins strategy to make a final prediction.

D. Complexity Analysis

Computational complexity is a significant metric to measure the amount of computing resources required for running a specific algorithm. Since the key processes of the proposed EVM-AMC method are the signal preprocessing and feature extraction, in this subsection, we quantify the computational complexity of our algorithm in terms of multiplication and comparison operations of these two processes. Besides, some discussions of the SVM complexity can be referred to the literature [47].

According to the Algorithm 1, the multiplication and comparison computational complexity (MCCC) of the signal preprocessing is determined by lines 1, 2, 3, and 8. It is clear that the MCCC involved in line 1 and 2 is $O(N_g)$ and $O(N)$, respectively. The FFT calculation of line 3 requires the MCCC of $O(N\log N)$. The MCCC of line 8 for self-circulant differential division is $O(N_e)$, where $N_e = 2SN/\rho$ is the length of the NNSQ sequence. As for the feature extraction module, the generation of matched error vectors requires the MCCC of $O(\sum_i^I M_i N_e)$, where M_i denotes the constellation number of the i^{th} NNSQCS mask. Then, the POF operation[3] requires the MCCC of $O(IN_e\log(N_q))$, where $N_q = N_eQ/100$. Moreover, the MCCC of the EVM feature extraction in terms of Eq. (15) is about $O(IN_f)$. It should be noted that N typically has the same order of magnitude as N_g, N_e, and N_f, but is much larger than I and N_q. Without loss of generality, the MCCC of the EVM-AMC can be simplified as $O(N(\log N + \sum_i^I M_i))$ when considering the signal preprocessing and feature extraction processes.

IV. Experimental Setup

In this section, we first configure the OFDM parameter settings utilized during the simulated dataset generation, where the synthetic effects of multipath fading channel, CFO, PO, and additive noise are considered. Then, we introduce some selected FB AMC methods for performance comparison. To evaluate the discussed advantages, both the probability

[3]This process can be deemed as the operation to find the top $Q\%$ values from N_e NNSQ elements.

TABLE I
THE MULTIPATH FADING CHANNEL CONDITIONS

Power \ Path Delay / Channel Type	50 ns	100 ns	150 ns	200 ns
Rician (K_f = 4)	0.90	0.10	–	–
Rayleigh	0.865	0.117	0.016	0.002

Notation: ns is the abbreviation of nanosecond.

of correct classification (P_{cc}) and the mean average accuracy (MAA) are employed as the performance metrics in this paper.

A. Dataset Description

In this subsection, we use the OFDM signal for dataset generation, where the length of subcarriers and CP are 256 and 64. The carrier frequency and the transmission bandwidth are set to 2.4GHz and 20MHz, respectively. The oversampling factor ρ is 4. We consider two sets of modulation types:

- **Simple set:** contains four simple modulation types including BPSK, QPSK, 16QAM, and 4ASK.
- **Complex set:** contains both the modulation types in simple set and additional six commonly used modulation types including 8PSK, 16PSK, 8QAM, 32QAM, 64QAM, and 8ASK.

For simulating the synthetic channel effects, the CFO value follows the uniform random distribution within $[-24\text{kHz}, 24\text{kHz}]$ and the PO value follows the same distribution within $[-\pi, \pi]$. Meanwhile, both the Rician and Rayleigh multipath fading channels are considered, where the Rician-K-factor of the first tap is set to 4 and the power delay profiles (PDP) are given in Table I. Notably, the channel coefficients are randomly and periodically regenerated during each OFDM symbol period.

A total of six datasets are generated via the combination of the modulation candidate sets (simple and complex sets) and channel conditions (AWGN, Rician, and Rayleigh) for performance evaluation. For ease of representation, we can write the generated datasets as $\mathcal{D}^S_{n_d}(n_d \in [1,2,3])$ for the simple set and $\mathcal{D}^C_{n_d}$ for the complex set, where the number of 1, 2 and 3 stands for the channel types of AWGN, Rician and Rayleigh, respectively. For each dataset, we generate 500 OFDM samples for each modulation type per SNR, with the SNR range of -10 dB to 20 dB (step is 2 dB). In other words, there are 32000 samples in $\mathcal{D}^S_{n_d}$ and 80000 samples in $\mathcal{D}^C_{n_d}$.

B. Baseline AMC Methods

For the purpose of performance comparison, we employ three baselines from the existing FB AMC methods, namely SaIF (statistical and instantaneous features) [18], HOC2 (two HOC features) [24], and SQ-HOC (spectral quotient-based HOC features) [36]. As demonstrated in [36], the SQ-HOC performs better when filtering out the outliers, thus we also employ a threshold-based outlier filter[4] in our following experiments. Besides, it should be noted that the HOC features employed in SaIF and HOC are extracted from the frequency-domain received signal after CFO compensation in this paper. Since the most complex operations in these baselines are the FFT calculations, their MCCC can be roughly deemed as $O(N \log N)$ without considering the classification process, which is slightly lower than the proposed EVM-AMC method (the MCCC is $O(N(\log N + \sum_i^I M_i))$).

In general, the classification performance can be affected by the adopted classifier. For fair comparisons, all these baselines employ the multi-class SVM classifier to distinguish the modulation types. LIBSVM [48] is a widely used open-source software library that provides implementations of SVM algorithms and is well-known for its efficiency and versatility in solving various machine learning problems. Therefore, we implement it to train the multi-class SVMs in this paper and the training settings are listed below: 1) the SVM type is C-SVC, 2) the kernel function is a polynomial base function, where the gamma is 15 and the degree is 2, 3) other hyperparameters are defaults.

[4]According to the reference [36], the threshold value employed at the signal preprocessing stage is set to 3.3 for outlier removal.

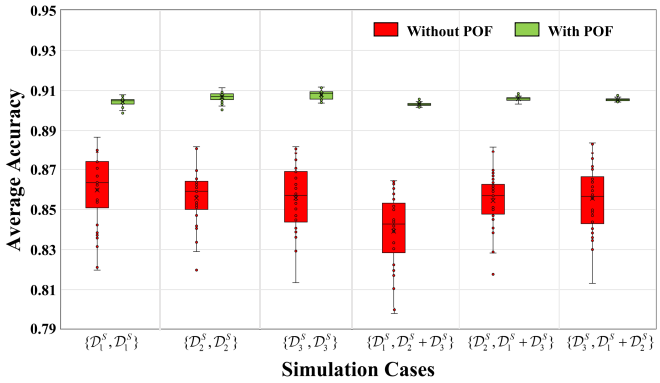

Fig. 4. The average accuracy results of the proposed method with/without percentile-based outlier filter using box plot.

C. Evaluation Metrics

To evaluate the classification performance, we employ the probability of correct classification with a specific SNR as a performance metric, which is calculated as

$$P_{cc}(z) = \sum_{i=1}^{I} P(\Theta_i, z) P(\hat{\Theta} = \Theta_i | \Theta_i, z), \tag{19}$$

where $P(\Theta_i, z)$ denotes the prior probability of modulation type Θ_i at the z^{th} SNR, $\hat{\Theta}$ represents the predicted modulation format and $P(\hat{\Theta} = \Theta_i | \Theta_i, z)$ stands for the conditional probability in the case that the modulation format is correctly predicted as Θ_i. Moreover, the MAA of all SNR variants is also employed as an evaluation metric, which is computed as

$$MAA = \frac{1}{Z} \sum_{z=1}^{Z} P_{cc}(z), \tag{20}$$

where Z is the total number of the SNR variants.

V. NUMERICAL RESULTS AND DISCUSSIONS

In this section, we investigate the classification performance of the proposed AMC method, where three parts are discussed.

Firstly, we study the influence of the percentile-based outlier filter on the classification performance of our method. Secondly, we compare the performance of the EVM-AMC methods with baselines using the datasets modulated with the simple set. Finally, we further compare the classification performance when the datasets modulated with the complex set are considered.

To study the channel effects on the AMC problem, we further divide the AMC tasks into two categories, i.e., homogeneous and heterogeneous tasks, which is explained as follows:

- Homogeneous AMC task: the channel conditions are constant during the training and testing stage.
- Heterogeneous AMC task: the channel conditions are changing during the training and testing stage.

When the homogeneous AMC task is considered, we divide the adopted dataset into the training set, validation set, and testing set in the ratio of 3:1:1. As for the heterogeneous AMC task, we divide the dataset employed in the training stage into training and validation sets in the ratio of 3:1, and the whole samples of the other two datasets with the same modulation candidate pool are used as testing sets. Besides, the maximum self-circulant shift step S and the percentile Q employed for the outlier filter are set to 4 and 2.5 in the signal preprocessing and feature extraction stages. Finally, Monte Carlo trials are carried out for the following experiments.

A. Effectiveness of the Percentile-Based Outlier Filter

To verify the effectiveness of the POF on the improvement of classification performance, we provide the accuracy results of the EVM-AMC method with and without the POF in both the homogeneous and heterogeneous AMC cases. For simplicity, we employ the symbol of $\{\mathcal{D}_x, \mathcal{D}_y\}$ to denote the AMC experiment that is trained on $\mathcal{D}_x$ and tested on $\mathcal{D}_y$ in the following.

As shown in Fig. 4, we use the box plot to express the simulation results of total 30 times. Obviously, two phenomena can be observed from this figure. One is that the worst performance with POF outperforms the best performance without POF for each case. Another is that the distribution of the average accuracy with POF (the gaps between the best and worst performance vary within 1%) is more steady than that without POF (the gaps between the best and worst performance vary from 5% to 8%). Moreover, to take a close look at the experiments, the MAA of these results is listed in Table II. As expected, the MAA results can be enhanced with the aid of the POF for each case. Specifically, the improvement of MAA is about 4.52% for $\{\mathcal{D}_1^S, \mathcal{D}_1^S\}$, 5.11% for $\{\mathcal{D}_1^S, \mathcal{D}_2^S\}$, 5.25% for $\{\mathcal{D}_1^S, \mathcal{D}_3^S\}$, 6.4% for $\{\mathcal{D}_1^S, \mathcal{D}_2^S + \mathcal{D}_3^S\}$, 5.15% for $\{\mathcal{D}_2^S, \mathcal{D}_1^S + \mathcal{D}_3^S\}$, 4.99% for $\{\mathcal{D}_3^S, \mathcal{D}_1^S + \mathcal{D}_2^S\}$. Hence, we can conclude that, for both the homogeneous and heterogeneous AMC tasks, the POF strategy is effective in improving the classification performance of the EVM-AMC method.

B. Performance Evaluation for the Homogeneous AMC Task

In this subsection, we first provide the P_{cc} curves when the homogeneous AMC task is considered. Fig. 5 provides the classification performance of the proposed method and all baselines on the simple modulation type set. As illustrated in these figures, the proposed EVM-AMC achieves the best performance under each channel condition when compared to the other three baselines, which can reach at least 95% accuracy at SNR $= -2$ dB. Moreover, the MAA results of both the EVM-AMC and SQ-HOC methods are almost unchanged (fluctuate within 0.5%) under different channel conditions, while the MAA results of the HOC2 and SaIF methods are highly related to the channel conditions. For example, when the modulated signals experience multipath fading effects, the MAA results of the HOC2 and SaIF methods significantly drop about 18.81% to 42.6% in comparison to the MAA results under AWGN channel. Meanwhile, the EVM-AMC method outperforms the SQ-HOC method by nearly 7% in MAA for each case.

Considering current wireless communication systems utilize a variety of modulation types, we further conduct the homogeneous experiments on the complex modulation type set, whose results are provided in Fig. 6. Again, the EVM-AMC achieves excellent MAA performance, which can identify the complex modulation types with an accuracy of more than 95% at SNR $= 10$ dB for each case. The accuracy of the SQ-HOC method is robust to the channel conditions, but it has a significant gap compared to the EVM-AMC method. The peak accuracy (at SNR $= 20$ dB) of the HOC2 is slightly less than 80% under AWGN channel, which means some modulation types cannot be classified well by this method. Besides, the HOC2 method performs poorly in the presence of channel effects, with a peak accuracy drop of 43% or so when compared to the result under AWGN channel. As for the SaIF method, it works effectively under AWGN channel, reaching the best MAA result (73.34%). However, this method performs less well under Rician and Rayleigh channels, which only achieves a peak accuracy of 50% to 56% in these cases. Thus, for the homogeneous AMC task, we can draw the following conclusions: 1) both the EVM-AMC and SQ-HOC methods are robust to different channel conditions, 2) the EVM-AMC method achieves excellent classification performance in both simple and complex modulation type sets, 3) the classification performance of the SQ-HOC and HOC2 methods is dependent on the channel conditions.

C. Performance Evaluation for the Heterogeneous AMC Task

In real-world wireless communication scenarios, the channel effects are constantly changing. It is very likely to encounter an unseen channel condition during the runtime. For evaluating the classification performance in such cases, we conduct the heterogeneous AMC experiments in this part. As revealed in Fig. 7, the proposed method yields the optimal classification performance, leading to at least 7.01%, 53%, and 42.15% MAA improvement with respect to the SQ-HOC, HOC2, and SaIF methods. Meanwhile, the SQ-HOC still performs effectively in these cases, but it performs less well than the EVM-AMC method in the low SNR region. As for the HOC2 and SaIF methods, they are ineffective when trained under AWGN channel but tested under Rician and Rayleigh channels. Even though their classification performance can be improved when trained on the samples impaired with channel

TABLE II
THE MAA RESULTS WITH AND WITHOUT THE PERCENTILE-BASED OUTLIER FILTER

MAA: Cases / Strategy	$\{\mathcal{D}_1^S, \mathcal{D}_1^S\}$	$\{\mathcal{D}_2^S, \mathcal{D}_2^S\}$	$\{\mathcal{D}_3^S, \mathcal{D}_3^S\}$	$\{\mathcal{D}_1^S, \mathcal{D}_2^S + \mathcal{D}_3^S\}$	$\{\mathcal{D}_2^S, \mathcal{D}_1^S + \mathcal{D}_3^S\}$	$\{\mathcal{D}_3^S, \mathcal{D}_1^S + \mathcal{D}_2^S\}$
Without POF	85.97%	85.57%	85.58%	83.91%	85.44%	85.55%
With POF	90.49% (4.52% ↑)	90.68% (5.11% ↑)	90.83% (5.25% ↑)	90.31% (6.40% ↑)	90.59% (5.15% ↑)	90.54% (4.99% ↑)

Notation: The red number denotes the MAA gap between two strategies.

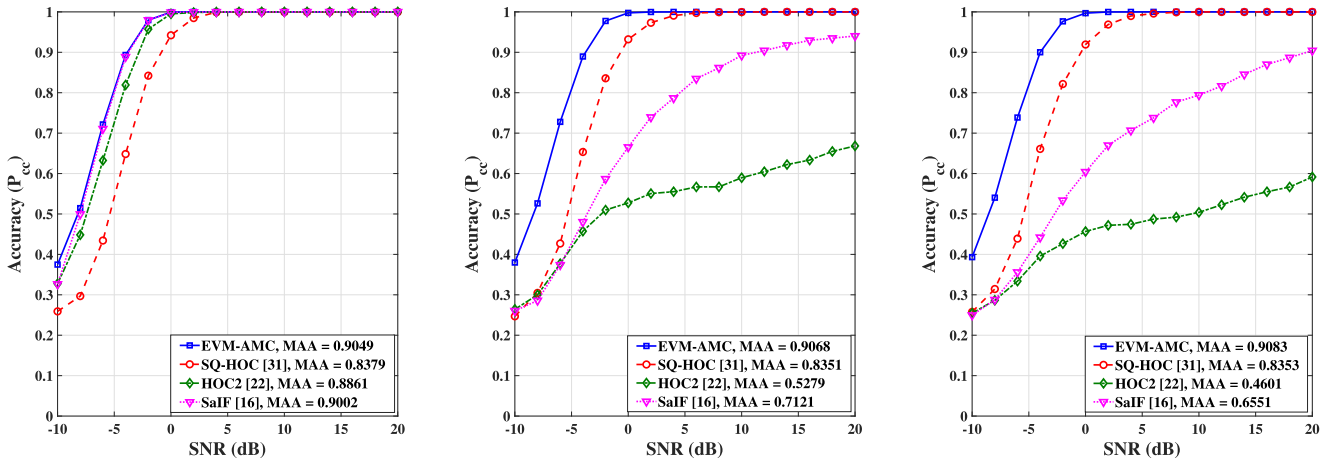

(a) (b) (c)

Fig. 5. Simple modulation type set: the performance comparison under different channel conditions when the homogeneous AMC task is considered. (a) Trained and tested on $\mathcal{D}_1^S$ (AWGN). (b) Trained and tested on $\mathcal{D}_2^S$ (Rician). (c) Trained and tested on $\mathcal{D}_3^S$ (Rayleigh).

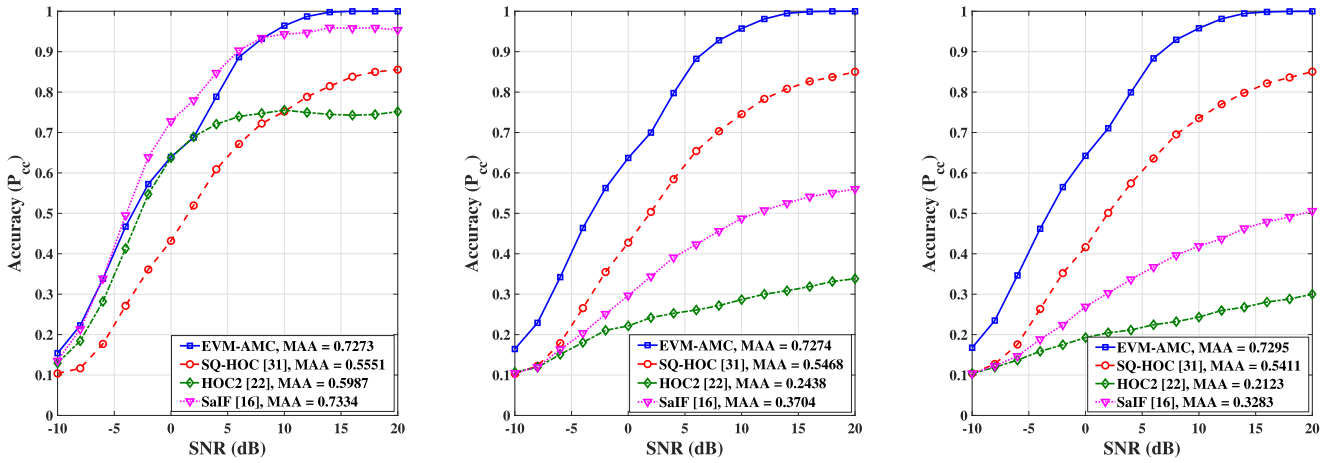

(a) (b) (c)

Fig. 6. Complex modulation type set: the performance comparison under different channel conditions when the homogeneous AMC task is considered. (a) Trained and tested on $\mathcal{D}_1^C$ (AWGN). (b) Trained and tested on $\mathcal{D}_2^C$ (Rician). (c) Trained and tested on $\mathcal{D}_3^C$ (Rayleigh).

effects, the overall accuracies of these methods fluctuate heavily and are still far away from a credible level. This can be attributed to the violation of the basic independent and identically distributed (i.i.d) assumption of machine learning, thus making the unclear predictions by the SVM classifiers in the heterogeneous cases.

Moreover, we also compare the classification performance of the proposed method with other baselines on the complex modulation type set. It can be appreciated from Fig. 8 that the EVM-AMC method consistently outperforms these baselines in each case. The SQ-HOC method only achieves a peak accuracy of about 85% at SNR = 20 dB, while our method can reach the same accuracy level at SNR = 6 dB. As expected, the HOC2 and SaIF methods perform poorly in these cases, reaching the MAA results of less than 25%. Hence, for the heterogeneous AMC task, we can conclude that 1) both the EVM-AMC and SQ-HOC methods exhibit extremely robustness and generalization, 2) the EVM-AMC method consistently outperforms these baselines in both simple and complex modulation type sets, 3) the HOC2 and SaIF methods can not accurately classify the modulation types when encountered the unseen channel conditions.

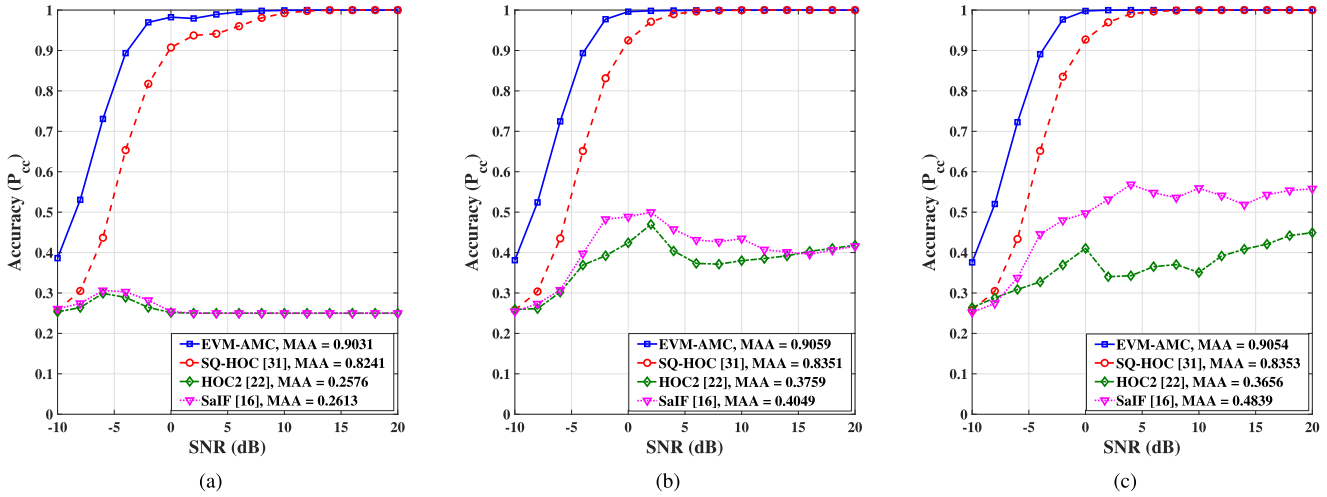

(a) (b) (c)

Fig. 7. Simple modulation type set: the performance comparison under different channel conditions when the heterogeneous AMC task is considered. (a) Trained on $\mathcal{D}_1^S$ (AWGN) and tested on $\mathcal{D}_2^S + \mathcal{D}_3^S$ (Rician + Rayleigh). (b) Trained on $\mathcal{D}_2^S$ (Rician) and tested on $\mathcal{D}_1^S + \mathcal{D}_3^S$ (AWGN + Rayleigh). (c) Trained on $\mathcal{D}_3^S$ (Rayleigh) and tested on $\mathcal{D}_1^S + \mathcal{D}_1^S$ (AWGN + Rician).

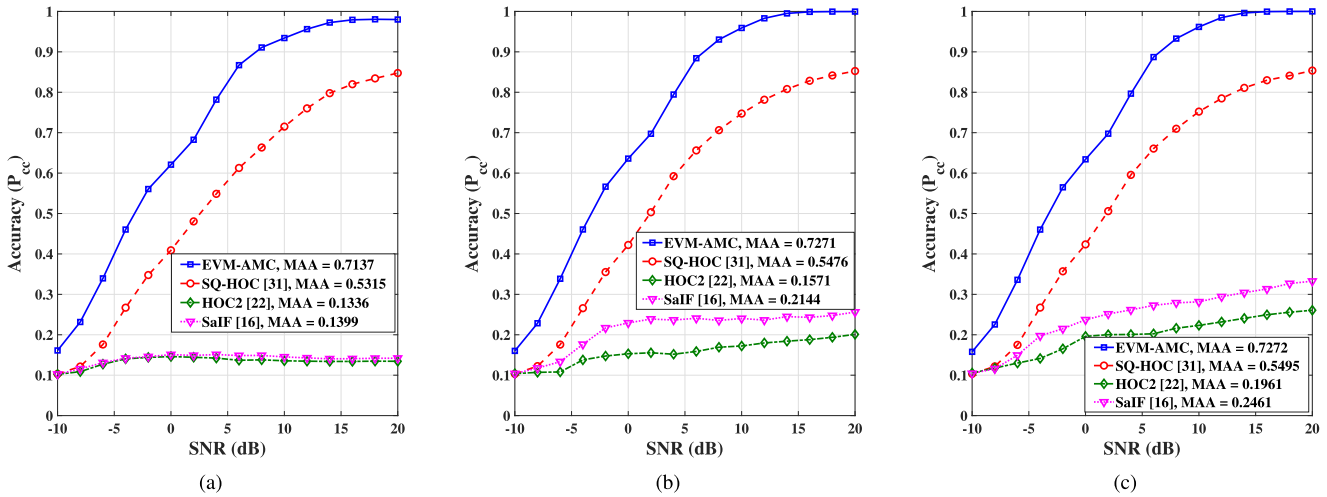

(a) (b) (c)

Fig. 8. Complex modulation type set: the performance comparison under different channel conditions when the heterogeneous AMC task is considered. (a) Trained on $\mathcal{D}_1^C$ (AWGN) and tested on $\mathcal{D}_2^C + \mathcal{D}_3^C$ (Rician + Rayleigh). (b) Trained on $\mathcal{D}_2^C$ (Rician) and tested on $\mathcal{D}_1^C + \mathcal{D}_3^C$ (AWGN + Rayleigh). (c) Trained on $\mathcal{D}_3^C$ (Rayleigh) and tested on $\mathcal{D}_1^C + \mathcal{D}_1^C$ (AWGN + Rician).

VI. Conclusion

In this paper, we presented an effective FB method, referred to as EVM-AMC, to identify the modulation types for OFDM systems in the presence of synthetic channel effects, i.e., multipath fading interferences, PO, CFO, and additive noise. To keep resistant to the synthetic channel effects, our method first performed the CFO compensation and then constructed the NNSQ sequence via the proposed AM-SCDD algorithm, where the PO and multipath fading effects can be jointly suppressed by this algorithm. Moreover, an EVM-based feature extractor was used to extract the modulation-specific features from the preprocessed signals. Finally, the collected features were sent to the multi-class SVM classifier module for training and testing. Experiments were conducted with two candidate modulation type pools for both the homogeneous and heterogeneous AMC tasks. Numerical results validated the superiority and robustness of the proposed EVM-AMC method when compared to other existing feature-based AMC methods under unknown synthetic channels.

The proposed method has the advantage of low computational complexity in comparision to the DL-based AMC method, which is suitable for practical deployment and application. When the computational resources are sufficient, the deep learning-based classifier can be used to pursue a high-accuracy performance. In the future, we will attempt to improve the classification performance at the low SNR regions for OFDM systems with more modulation types.

References

[1] S. Peng, S. Sun, and Y.-D. Yao, "A survey of modulation classification using deep learning: Signal representation and data preprocessing," *IEEE Trans. Neural Netw. Learn. Syst.*, vol. 33, no. 12, pp. 7020–7038, Dec. 2022.

[2] S. Hanna, C. Dick, and D. Cabric, "Signal processing-based deep learning for blind symbol decoding and modulation classification," *IEEE J. Sel. Areas Commun.*, vol. 40, no. 1, pp. 82–96, Jan. 2022.

[3] R. Gupta, S. Majhi, and O. A. Dobre, "Design and implementation of a tree-based blind modulation classification algorithm for multiple-antenna systems," *IEEE Trans. Instrum. Meas.*, vol. 68, no. 8, pp. 3020–3031, Aug. 2019.

[4] W. Chen, Z. Xie, L. Ma, J. Liu, and X. Liang, "A faster maximum-likelihood modulation classification in flat fading non-Gaussian channels," *IEEE Commun. Lett.*, vol. 23, no. 3, pp. 454–457, Mar. 2019.

[5] A. P. Hermawan, R. R. Ginanjar, D. Kim, and J. Lee, "CNN-based automatic modulation classification for beyond 5G communications," *IEEE Commun. Lett.*, vol. 24, no. 5, pp. 1038–1041, May 2020.

[6] F. Hameed, O. A. Dobre, and D. C. Popescu, "On the likelihood-based approach to modulation classification," *IEEE Trans. Wireless Commun.*, vol. 8, no. 12, pp. 5884–5892, Dec. 2009.

[7] J. Zhang, D. Cabric, F. Wang, and Z. Zhong, "Cooperative modulation classification for multipath fading channels via expectation-maximization," *IEEE Trans. Wireless Commun.*, vol. 16, no. 10, pp. 6698–6711, Oct. 2017.

[8] N. Jafar, A. Paeiz, and A. Farzaneh, "Automatic modulation classification using modulation fingerprint extraction," *J. Syst. Eng. Electron.*, vol. 32, no. 4, pp. 799–810, Aug. 2021.

[9] D. Grimaldi, S. Rapuano, and L. D. Vito, "An automatic digital modulation classifier for measurement on telecommunication networks," *IEEE Trans. Instrum. Meas.*, vol. 56, no. 5, pp. 1711–1720, Oct. 2007.

[10] A. Ramezani-Kebrya, I. Kim, D. I. Kim, F. Chan, and R. Inkol, "Likelihood-based modulation classification for multiple-antenna receiver," *IEEE Trans. Commun.*, vol. 61, no. 9, pp. 3816–3829, Sep. 2013.

[11] K. Qiu, S. Zheng, L. Zhang, C. Lou, and X. Yang, "DeepSIG: A hybrid heterogeneous deep learning framework for radio signal classification," *IEEE Trans. Wireless Commun.*, vol. 23, no. 1, pp. 775–788, Jan. 2024.

[12] S. Chang, S. Huang, R. Zhang, Z. Feng, and L. Liu, "Multitask-Learning-based deep neural network for automatic modulation classification," *IEEE Internet Things J.*, vol. 9, no. 3, pp. 2192–2206, Feb. 2022.

[13] R. Zhang, Y. Zhao, Z. Yin, D. Li, and Z. Wu, "A reference signal-aided deep learning approach for overlapped signals automatic modulation classification," *IEEE Commun. Lett.*, vol. 27, no. 4, pp. 1135–1139, Apr. 2023.

[14] S. Chang, Z. Yang, J. He, R. Li, S. Huang, and Z. Feng, "A fast multi-loss learning deep neural network for automatic modulation classification," *IEEE Trans. Cognit. Commun. Netw.*, vol. 9, no. 6, pp. 1503–1518, Dec. 2023.

[15] S. Majhi, R. Gupta, W. Xiang, and S. Glisic, "Hierarchical hypothesis and feature-based blind modulation classification for linearly modulated signals," *IEEE Trans. Veh. Technol.*, vol. 66, no. 12, pp. 11057–11069, Dec. 2017.

[16] A. K. Nandi and E. E. Azzouz, "Algorithms for automatic modulation recognition of communication signals," *IEEE Trans. Commun.*, vol. 46, no. 4, pp. 431–436, Apr. 1998.

[17] S. Huang, Y. Yao, Z. Wei, Z. Feng, and P. Zhang, "Automatic modulation classification of overlapped sources using multiple cumulants," *IEEE Trans. Veh. Technol.*, vol. 66, no. 7, pp. 6089–6101, Jul. 2017.

[18] B. Luo, Q. Peng, P. C. Cosman, and L. B. Milstein, "Robustness of deep modulation recognition under AWGN and Rician fading," in *Proc. 52nd Asilomar Conf. Signals, Syst., Comput.*, Pacific Grove, CA, USA, Oct. 2018, pp. 447–450.

[19] S. Chang, R. Zhang, K. Ji, S. Huang, and Z. Feng, "A hierarchical classification head based convolutional gated deep neural network for automatic modulation classification," *IEEE Trans. Wireless Commun.*, vol. 21, no. 10, pp. 8713–8728, Oct. 2022.

[20] W. U. Bajwa, J. Haupt, A. M. Sayeed, and R. Nowak, "Compressed channel sensing: A new approach to estimating sparse multipath channels," *Proc. IEEE*, vol. 98, no. 6, pp. 1058–1076, Jun. 2010.

[21] Y. Liu, Z. Tan, H. Hu, L. J. Cimini, and G. Y. Li, "Channel estimation for OFDM," *IEEE Commun. Surveys Tuts.*, vol. 16, no. 4, pp. 1891–1908, 4th Quart., 2014.

[22] P. Zhang, L. Li, K. Niu, Y. Li, G. Lu, and Z. Wang, "An intelligent wireless transmission toward 6G," *Intell. Converged Netw.*, vol. 2, no. 3, pp. 244–257, Sep. 2021.

[23] S. Chang, S. Huang, R. Zhang, Z. Feng, and L. Liu, "Multitask-learning-based deep neural network for automatic modulation classification," *IEEE Internet Things J.*, vol. 9, no. 3, pp. 2192–2206, Feb. 2022.

[24] A. Swami and B. M. Sadler, "Hierarchical digital modulation classification using cumulants," *IEEE Trans. Commun.*, vol. 48, no. 3, pp. 416–429, Mar. 2000.

[25] X. Zhang et al., "NAS-AMR: Neural architecture search-based automatic modulation recognition for integrated sensing and communication systems," *IEEE Trans. Cogn. Commun. Netw.*, vol. 8, no. 3, pp. 1374–1386, Sep. 2022.

[26] R. R. Yakkati, R. R. Yakkati, R. K. Tripathy, and L. R. Cenkeramaddi, "Radio frequency spectrum sensing by automatic modulation classification in cognitive radio system using multiscale deep CNN," *IEEE Sensors J.*, vol. 22, no. 1, pp. 926–938, Jan. 2022.

[27] F. Wang and X. Wang, "Fast and robust modulation classification via Kolmogorov-Smirnov test," *IEEE Trans. Commun.*, vol. 58, no. 8, pp. 2324–2332, Aug. 2010.

[28] Y. Du, G. Zhu, J. Zhang, and K. Huang, "Automatic recognition of space-time constellations by learning on the Grassmann manifold," *IEEE Trans. Signal Process.*, vol. 66, no. 22, pp. 6031–6046, Nov. 2018.

[29] S. Hong, Y. Zhang, Y. Wang, H. Gu, G. Gui, and H. Sari, "Deep learning-based signal modulation identification in OFDM systems," *IEEE Access*, vol. 7, pp. 114631–114638, 2019.

[30] T. Huynh-The, Q.-V. Pham, T.-V. Nguyen, X.-Q. Pham, and D.-S. Kim, "Deep learning-based automatic modulation classification for wireless OFDM communications," in *Proc. Int. Conf. Inf. Commun. Technol. Converg. (ICTC)*, Oct. 2021, pp. 47–49.

[31] P. Shih and D. Chang, "An automatic modulation classification technique using high-order statistics for multipath fading channels," in *Proc. 11th Int. Conf. ITS Telecommun.*, Aug. 2011, pp. 691–695.

[32] Y. Wang et al., "Automatic modulation classification for MIMO systems via deep learning and zero-forcing equalization," *IEEE Trans. Veh. Technol.*, vol. 69, no. 5, pp. 5688–5692, May 2020.

[33] R. Gupta, S. Kumar, and S. Majhi, "Blind modulation classification for asynchronous OFDM systems over unknown signal parameters and channel statistics," *IEEE Trans. Veh. Technol.*, vol. 69, no. 5, pp. 5281–5292, May 2020.

[34] T. Huynh-The, T. Nguyen, Q. Pham, D. B. Da Costa, G. Kwon, and D. Kim, "Efficient convolutional networks for robust automatic modulation classification in OFDM-based wireless systems," *IEEE Syst. J.*, vol. 17, no. 1, pp. 964–975, Mar. 2023.

[35] E. Perenda, S. Rajendran, G. Bovet, S. Pollin, and M. Zheleva, "Learning the unknown: Improving modulation classification performance in unseen scenarios," in *Proc. INFOCOM IEEE Conf. Comput. Commun.*, Vancouver, BC, Canada, May 2021, pp. 1–10.

[36] S. Huang, Y. Chen, J. He, S. Chang, and Z. Feng, "Channel-robust automatic modulation classification using spectral quotient cumulants," 2023, *arXiv:2310.08021*.

[37] J. He, S. Huang, S. Chang, F. Wang, B.-Z. Shen, and Z. Feng, "Radio frequency fingerprint identification with hybrid time-varying distortions," *IEEE Trans. Wireless Commun.*, vol. 22, no. 10, pp. 6724–6736, Feb. 2023.

[38] L. Li, Y. Wang, and L. Ding, "On the bit error probability of OFDM and FBMC-OQAM systems in Rayleigh and Rician multipath fading channels," *IEICE Trans. Commun.*, vol. 102, no. 12, pp. 2276–2285, Dec. 2019.

[39] T. Yucek and H. Arslan, "OFDM signal identification and transmission parameter estimation for cognitive radio applications," in *Proc. IEEE GLOBECOM Global Telecommun. Conf.*, Washington, DC, USA, Nov. 2007, pp. 4056–4060.

[40] P. K. Nishad and P. Singh, "Carrier frequency offset estimation in OFDM systems," in *Proc. IEEE Conf. Inf. Commun. Technol.*, Thuckalay, India, Apr. 2013, pp. 885–889.

[41] J. He, S. Huang, Z. Yang, K. Yu, H. Huan, and Z. Feng, "Channel-agnostic radio frequency fingerprint identification using spectral quotient constellation errors," *IEEE Trans. Wireless Commun.*, vol. 23, no. 1, pp. 158–170, Jan. 2024.

[42] C. Zhao and R. J. Baxley, "Error vector magnitude analysis for OFDM systems," in *Proc. 14th Asilomar Conf. Signals Syst. Comput.*, Pacific Grove, CA, USA, 2006, pp. 1830–1834.

[43] J. Cervantes, F. Garcia-Lamont, L. Rodríguez-Mazahua, and A. Lopez, "A comprehensive survey on support vector machine classification: Applications, challenges and trends," *Neurocomputing*, vol. 408, pp. 189–215, Sep. 2020.

[44] B. E. Boser, I. M. Guyon, and V. N. Vapnik, "A training algorithm for optimal margin classifiers," in *Proc. 5th Annu. Workshop Comput. Learn. Theory*, Pittsburgh, PA, USA, 1992, pp. 144–152.

[45] C.-W. Hsu and C.-J. Lin, "A comparison of methods for multiclass support vector machines," *IEEE Trans. Neural Netw.*, vol. 13, no. 2, pp. 415–425, Mar. 2002.

[46] Y. Tian, Z. Qi, X. Ju, Y. Shi, and X. Liu, "Nonparallel support vector machines for pattern classification," *IEEE Trans. Cybern.*, vol. 44, no. 7, pp. 1067–1079, Jul. 2014.

[47] A. Abdiansah and R. Wardoyo, "Time complexity analysis of support vector machines (SVM) in LibSVM," *Int. J. Comput. Appl.*, vol. 128, no. 3, pp. 28–34, 2015.

[48] C.-C. Chang and C.-J. Lin, "LIBSVM: A library for support vector machines," *ACM Trans. Intell. Syst. Technol.*, vol. 2, no. 3, pp. 1–27, Apr. 2011.

Sai Huang (Senior Member, IEEE) is currently with the Department of Information and Communication Engineering, Beijing University of Posts and Telecommunications, as an Associate Professor, and serves as the Academic Secretary of the Key Laboratory of Universal Wireless Communications, Ministry of Education, China. He is a reviewer of international journals, such as IEEE TRANSACTIONS ON WIRELESS COMMUNICATIONS, IEEE TRANSACTIONS ON VEHICULAR TECHNOLOGY, IEEE WIRELESS COMMUNICATIONS LETTERS, and IEEE TRANSACTIONS ON COGNITIVE COMMUNICATIONS AND NETWORKING, and international conferences, such as IEEE ICC and IEEE GLOBECOM. His research interests include machine learning-assisted intelligent signal processing, statistical spectrum sensing and analysis, fast detection and depth recognition of universal wireless signals, millimeter wave signal processing, and cognitive radio networks.

Jiashuo He (Graduate Student Member, IEEE) received the M.S. degree in communication engineering from Xidian University, Xi'an, China, in 2021. He is currently pursuing the Ph.D. degree with Beijing University of Posts and Telecommunications, Beijing, China. His current research interests include signal processing, automatic modulation classification, and radio frequency fingerprint identification.

Zheng Yang received the B.S. degree from Beijing University of Posts and Telecommunications, Beijing, China, in 2020, where he is currently pursuing the Ph.D. degree. His current research interests include automatic modulation classification and security in 5G/B5G.

Yuting Chen received the B.S. degree from North China University of Technology, Beijing, China, in 2022. She is currently pursuing the M.S. degree with Beijing University of Posts and Telecommunications, Beijing. Her current research interests include signal processing, automatic modulation classification, deep learning, and radio frequency fingerprint identification.

Shuo Chang (Member, IEEE) received the B.S. degree in communication engineering from Shenyang Jianzhu University, Shenyang, China, in 2015, and the Ph.D. degree from Beijing University of Posts and Telecommunications (BUPT), Beijing, China, in 2020. He is currently a Post-Doctoral Researcher with BUPT. He is also a member of the Key Laboratory of Universal Wireless Communications, Ministry of Education, China. His research interests include signal processing, visual object tracking, visual detection, and sensor fusion.

Yifan Zhang received the B.S., M.S., and Ph.D. degrees from Beijing University of Posts and Telecommunications (BUPT). He is currently a Researcher with the School of Information and Communication Engineering, BUPT. His current research interests include signal modulation classification, signal processing, cognitive radio network implementation, and optimization algorithms in wireless networks.

Zhiyong Feng (Senior Member, IEEE) received the B.S., M.S., and Ph.D. degrees in information and communication engineering from Beijing University of Posts and Telecommunications (BUPT), Beijing, China. She is currently a Full Professor. She is also the Director of the Key Laboratory of Universal Wireless Communications, Ministry of Education. Her research interests include wireless network architecture design and radio resource management in 5th-generation mobile networks (5G), spectrum sensing and dynamic spectrum management in cognitive wireless networks, universal signal detection and identification, and network information theory. She is a Technical Advisor of NGMN; an editor of *IET Communications* and *KSII Transactions on Internet and Information Systems*; and a reviewer of IEEE TRANSACTIONS ON WIRELESS COMMUNICATIONS, IEEE TRANSACTIONS ON VEHICULAR TECHNOLOGY, and IEEE JOURNAL ON SELECTED AREAS IN COMMUNICATIONS. She is active in ITU-R, IEEE, ETSI, and CCSA standards.